Preprint typeset in JHEP style. - HYPER VERSION

MIT-CTP-3290, NI02015-MTH, hep-th/0207132

Perturbative diagrams in string field theory

Washington Taylor

Center for Theoretical Physics
MIT, Bldg. 6-308
Cambridge, MA 02139, U.S.A.
wati@mit.edu

Abstract: A general algorithm is presented which gives a closed-form expression for an arbitrary perturbative diagram of cubic string field theory at any loop order. For any diagram, the resulting expression is given by an integral of a function of several infinite matrices, each built from a finite number of blocks containing the Neumann coefficients of Witten's 3-string vertex. The closed-form expression for any diagram can be approximated by level truncation on oscillator level, giving a computation involving finite size matrices. Some simple tree and loop diagrams are worked out as examples of this approach.

Keywords: String field theory.

Contents

1. Perturbative diagrams in string field theory

1.1. Introduction

String field theory is a formulation of string theory as a nonlocal field theory of an infinite number of fields in space-time. This approach goes beyond the world-sheet formulation of string theory in several ways. First, it gives a systematic way of constructing perturbative string amplitudes in terms of vertices and propagators; this approach is in principle easier to generalize to higher loop amplitudes than the world-sheet approach, which involves conformal field theory on higher genus Riemann surfaces. Second, string field theory gives a nonperturbative off-shell formulation of string theory, and can be used to address questions which go beyond string perturbation theory. Third, while all current formulations of string field theory are formally described in a fixed string background, fluctuations of the string background itself are naturally encoded in the theory, so that string field theory is really a background-independent theory. Recent work using Witten's cubic open string field theory [1] to confirm Sen's conjectures [2] regarding tachyon condensation has demonstrated conclusively that string field theory accurately describes some nonperturbative off-shell aspects of string physics (for reviews see [3, 4, 5]). Furthermore, the existence of a nontrivial vacuum solution of string field theory demonstrates the background independence of the theory [6, 7, 8].

In this paper we focus on the first of the points mentioned in the previous paragraph, namely the construction of arbitrary perturbative string amplitudes using string field theory. Constructing higher-loop amplitudes in string theory using covariant world-sheet methods becomes difficult when the Riemann surface involved has genus greater than one. This is because the calculation of a generic string amplitude involves an integral over the moduli space of the appropriate Riemann surface, and it is difficult to define an appropriate measure on the moduli space for higher-genus surfaces. On the other hand, a string field theory such as Witten's cubic open string field theory gives a straightforward construction, in principle, of any higher-loop amplitude. The amplitude can be expressed in standard field-theoretic language in terms of the cubic vertices and the propagators for the infinite number of space-time fields. The difficulty with doing such a calculation explicitly is that the infinite number of fields have complicated cubic interactions described by the Witten 3-string vertex.

Formal arguments have demonstrated that in a particular gauge (Feynman-Siegel gauge), Witten's cubic bosonic open string field theory gives rise to a diagrammatic expansion which precisely covers the moduli space of Riemann surfaces of arbitrary genus with at least one boundary and with an arbitrary number of open string punctures on the boundaries [9, 10]. These results show that this string field theory must precisely reproduce all perturbative on-shell string amplitudes given by the conformal field theory of the bosonic string in 26 dimensions. Explicit computations of perturbative amplitudes using string field theory, however, have only been done for the tree level 4-point function and the one-loop 2-point function [11, 12, 13, 14]. These computations were done using the conformal mapping method, and required an explicit mapping between the modular parameters associated with the string field theory parameterization of moduli space and the standard parameterization of conformal field theory. Such mappings lead to complicated formulae even for tree-level and genus one calculations, and are unknown beyond genus one.

In this paper, we take a different approach to reproducing perturbative string amplitudes from string field theory. Rather than trying to relate string field theory calculations to conformal field theory, we simply proceed directly to evaluate perturbative amplitudes using the oscillator representation of the vertices and propagators in Witten's cubic string field theory. Since the vertex and propagator can be written completely in terms of squeezed states, we can give a closed-form expression for any perturbative amplitude, even at higher loop order. The only complication is the appearance of infinite-dimensional matrices in the final expression for each diagram. These matrices are built from simple blocks, however, which can be expressed in terms of the Neumann coefficient of Witten's 3-string vertex. While we do not yet have the technology to analytically evaluate amplitudes written in terms of these matrices, we can evaluate any desired amplitude numerically to a high degree of precision using truncation on the level of oscillators which are included. This truncation method is more powerful than the method of level truncation on fields used to address the tachyon condensation problem in [6, 7, 15, 8], since rather than having to include a number of fields which grows exponentially in the level, we simply need to evaluate the determinant of some matrices whose size grows linearly in the truncation level.

In Section 1.2 we give a brief review of Witten's cubic open string field theory to fix notation. In Section 1.3 we present an algorithm for computing a closed-form expression for any perturbative string amplitude. Section 2 contains a number of examples of tree- and loop-level diagrams: at tree level we analyze the 4-point and 5-point functions for the tachyon, at one loop we describe the tadpole, and at two loops we describe the 0-point function. We perform numerical evaluations of some of these amplitudes, showing that the procedure of level convergence on oscillator level (amounting to a sort of UV cutoff from the open string point of view) converges quickly.

1.2. Witten's cubic string field theory

In this subsection we give a brief synopsis of Witten's cubic string field theory [1]. For further

background on open string field theory see [1, 16, 17].

The degrees of freedom of Witten's cubic string field theory are encoded in a string field Φ. Φ can be considered as a functional $\Phi[x(\sigma); c(\sigma), b(\sigma)]$ of the matter, ghost, and antighost configuration of the string. Φ can also be thought of as living in the string Fock space $\mathcal{H}$ spanned by states produced by acting with a finite number of oscillators on the string vacuum

$$\Phi = \int d^{26}p \ [\phi(p) \ |0;p\rangle + A_\mu(p) \ \alpha_{-1}^\mu |0;p\rangle + \cdots] \ . \tag{1.1}$$

In this expression, $|0;p\rangle$ is the ghost number 1 vacuum at momentum p, which is annihilated by matter, antighost, and ghost modes a_n, b_n, c_n with $n \geq 1$. In this paper we use matter oscillators with canonical commutation relations $[a_n, a_{-m}] = \delta_{nm}$.

The action of Witten's theory can be written

$$S = -\frac{1}{2}\langle V_2|\Phi, Q\Phi\rangle - \frac{g}{3}\langle V_3|\Phi,\Phi,\Phi\rangle \tag{1.2}$$

where $|V_2\rangle \in \mathcal{H}^2, |V_3\rangle \in \mathcal{H}^3$. Explicit oscillator representations of $|V_2\rangle, |V_3\rangle$ are given by

$$|V_2\rangle = \int d^{26}p \ \exp\left(-a_{-n}^{(1)} C_{nm} a_{-m}^{(2)} - c_{-n}^{(1)} C_{nm} b_{-m}^{(2)} - c_{-n}^{(2)} C_{nm} b_{-m}^{(1)}\right) \times \tag{1.3}$$
$$(c_0^{(1)} + c_0^{(2)}) \ (|0;p\rangle \otimes |0;-p\rangle)$$

$$|V_3\rangle = \int d^{26}p^{(1)} \, d^{26}p^{(2)} \ \exp\left(-\frac{1}{2}a_{-n}^{(i)} N_{nm}^{ij} a_{-m}^{(j)} - a_{-n}^{(i)} N_{n0}^{ij} p^{(j)} - \frac{1}{2}p^{(i)} N_{00}^{ij} p^{(j)} - c_{-n}^{(i)} X_{nm}^{ij} b_{-m}^{(j)}\right) \times$$
$$(c_0^{(1)} c_0^{(2)} c_0^{(3)}) \left(|0;p^{(1)}\rangle \otimes |0;p^{(2)}\rangle \otimes |0;p^{(3)} = -p^{(1)} - p^{(2)}\rangle)\right) \tag{1.4}$$

where Q is the open string BRST operator,

$$C_{nm} = \delta_{nm}(-1)^n \, , \tag{1.5}$$

and where N_{nm}^{ij}, X_{nm}^{ij} are Neumann coefficients for which exact expressions are given in [18, 19, 20, 21]. The values of these coefficients are tabulated for $n + m < 10$ in [15]. (Note that with the conventions we are using here, the Neumann coefficients N_{nm}^{ij} in that reference should be rescaled by factors of $-\sqrt{nm}$. We have also removed from $|V_3\rangle$ an overall numerical factor of $k = (3\sqrt{3}/2)^3$. Note also that in (1.3, 1.4), all summations over indices n, m are taken over $n, m \geq 1$, except the last summation over m, which is taken over $m \geq 0$ so that the mode b_0 is included.)

The action (1.2) has an enormous gauge symmetry. A convenient choice of gauge for perturbative calculations is Feynman-Siegel gauge, where $b_0|\Phi\rangle = 0$. In this gauge, all fields associated with states having a c_0 acting on the vacuum are taken to vanish. This simplifies the above vertices in that we can ignore all ghost 0 modes c_0, b_0. Furthermore, the BRST operator in this gauge is simply

$$Q = c_0 L_0 = c_0(p^2 + N^{(m)} + N^{(g)} - 1) \, . \tag{1.6}$$

All calculations in this paper are done in Feynman-Siegel gauge. In this gauge the propagator is given by (dropping the factor of c_0)

$$\frac{1}{L_0} = \int_0^\infty dT \ e^{-TL_0} \, . \tag{1.7}$$

1.3. Algorithm for computing amplitudes

We now present a general algorithm which gives a closed-form expression for any perturbative open string diagram in Feynman-Siegel gauge. A number of examples are worked out explicitly in the following section.

Consider any diagram with v cubic vertices and e internal edges. Label the half-edges in the diagram with integers from 1 through $3v$, with labels 1, 2, 3 for the half-edges connected to vertex 1, labels 4, 5, 6 for the half-edges connected to vertex 2, and so forth. Denote the half-edges associated with the kth internal edge by i_k, j_k, so that the first edge connects the half-edges i_1, j_1, etc. The v 3-string vertices can be represented in the $3v$-fold tensor product of the single string Fock space through

$$|V\rangle = |V_3\rangle_{123} \otimes |V_3\rangle_{456} \otimes \cdots \otimes |V_3\rangle_{(3v-2)(3v-1)(3v)} \in \mathcal{H}^{3v} . \tag{1.8}$$

The propagator in Feynman-Siegel gauge for the e internal edges can be written by acting with half of each propagator on each associated half-edge, giving an operator on $\mathcal{H}^{3v}$

$$P = \int \prod_{k=1}^{e} dT_k \; e^{-\frac{1}{2}T_k(2p_k^2 + N_{i_k} + N_{j_k} - 2)} . \tag{1.9}$$

The constraint that the half-edges i_k, j_k are connected can be simply imposed by contracting with the dual state

$$\langle D| = \left(\prod_{k=1}^{e} \int d^{26}p \; \langle p_{i_k} = p| \otimes \langle p_{j_k} = -p| \right) \times \tag{1.10}$$
$$\exp\left(\sum_{k=1}^{e} -a_n^{(i_k)} C_{nm} a_m^{(j_k)} - c_n^{(i_k)} C_{nm} b_m^{(j_k)} - c_n^{(j_k)} C_{nm} b_m^{(i_k)} \right) .$$

We drop all factors of c_0, b_0 from (1.8) and (1.10) as they automatically cancel for calculations in Feynman-Siegel gauge. The full amplitude for the diagram under consideration is now given by an integral over internal (loop) momenta

$$\mathcal{A} = \int \prod_{i=1}^{1+e-v} d^{26}q_i \; \langle D|P|V\rangle . \tag{1.11}$$

This amplitude is a state in $\mathcal{H}^{3v-2e}$, and can be contracted with any external string states to get any particular amplitude associated with the relevant diagram.

Since all the pieces of (1.11) are given in terms of exponentials of quadratic expressions in the oscillators, we can give a closed form expression for any diagram using standard squeezed state techniques. It is convenient to first compute $P|V\rangle$, which is given by

$$P|V\rangle = \int \prod_{k=1}^{e} (dT_k e^{T_k(1-p_k^2)}) \times \tag{1.12}$$
$$\exp\left(-\frac{1}{2} a_{-n}^{(i)} \tilde{N}_{nm}^{ij} a_{-m}^{(j)} - a_{-n}^{(i)} \tilde{N}_{n0}^{ij} p^{(j)} - \frac{1}{2} p^{(i)} N_{00}^{ij} p^{(j)} - c_{-n}^{(i)} \tilde{X}_{nm}^{ij} b_{-m}^{(j)} \right) \left(\prod_{i=1}^{3v} |p_i\rangle \right) ,$$

where $\tilde{N}$ is a block-diagonal matrix consisting of 3 by 3 blocks of infinite matrices N^{rs} of Neumann coefficients associated with each 3-string vertex, multiplied by an exponential factor for the appropriate propagator(s). For a pair of internal indices i_k, j_l at a common vertex, we have

$$\tilde{N}^{i_k j_l}_{nm} = \hat{N}^{ij}_{nm}(e^{-T_k}, e^{-T_l}) \equiv e^{-nT_k/2} N^{ij}_{nm} e^{-mT_l/2}, \tag{1.13}$$

where i, j are equal to i_k, j_l modulo 3. For indices at a given vertex associated with external edges, the exponential factors are dropped, which can be expressed by replacing the relevant argument(s) of $\hat{N}$ by 1. The matrix $\tilde{X}$ is similarly constructed from the ghost Neumann coefficients X^{ij}_{mn} of the Witten vertex. We can now remove all oscillators associated with internal edges using the matter equation [22]

$$\begin{aligned} &\langle 0| \exp\left(-\frac{1}{2} a \cdot S \cdot a\right) \exp\left(-\mu \cdot a^\dagger - \frac{1}{2} a^\dagger \cdot \tilde{N} \cdot a^\dagger\right) |0\rangle \\ &\qquad = \frac{1}{\det(1 - S\tilde{N})^{1/2}} \exp\left(-\frac{1}{2} \mu \cdot (1 - S\tilde{N})^{-1} S \cdot \mu\right) \end{aligned} \tag{1.14}$$

and the associated ghost equation

$$\begin{aligned} &\langle 0| \exp\left(-c \cdot S \cdot b\right) \exp\left(-\lambda_c \cdot b^\dagger - c^\dagger \cdot \lambda_b - c^\dagger \cdot \tilde{X} \cdot b^\dagger\right) |0\rangle \\ &\qquad = \det(1 + S\tilde{X}) \exp\left(-\lambda_c \cdot (1 - S\tilde{X})^{-1} S \cdot \lambda_b\right) . \end{aligned} \tag{1.15}$$

This gives us an expression for the diagram of interest in terms of an integral over internal momenta and moduli of the form

$$\begin{aligned} \mathcal{A} = \int \left(\prod_{i=1}^{1+e-v} d^{26} q_i\right) \left(\prod_{k=1}^{e} dT_k \, e^{T_k}\right) \frac{\det(1 + S\tilde{X})}{\det(1 - S\tilde{N})^{13}} \\ \times \exp\left(-\frac{1}{2}(a^\dagger, p_i) \cdot Q \cdot (a^\dagger, p_i) - c^\dagger \cdot R \cdot b^\dagger\right) \left(\prod_{i=1}^{3v-2e} |p_i\rangle\right) . \end{aligned} \tag{1.16}$$

In this expression, $\tilde{X}$ and $\tilde{N}$ are as above, and depend on the modular parameters T_i. The determinants are evaluated in the $2e \times \infty$ dimensional space associated with internal edges. The 0 components of these matrices associated with momentum are not included in the determinant; all momentum factors are left explicitly in the exponential. The matrix S is simply a permutation matrix expressing which half-edges are connected by propagators, tensored with the infinite matrix C. The oscillators $a^\dagger, b^\dagger, c^\dagger$ are the raising operators associated with matter, antighost and ghost fields of the external edges; the notation $(a^\dagger, p_i)$ indicates a vector including the matter raising operators of external edges, as well as all external and internal momenta. The quadratic forms Q and R are matrices depending on the modular parameters T_i; these quadratic forms take the schematic form $N + N(1 - S\tilde{N})^{-1} SN$ and $X + X(1 - S\tilde{X})^{-1} SX$. Since all integrals over the internal momenta q_i are Gaussian, these can be readily performed, leaving an integral over the modular parameters associated with the edge lengths T_i.

This completes the algorithm for constructing a closed-form expression for any perturbative string diagram using Witten's cubic string field theory. A number of examples are

worked out explicitly in the following section, which should help to clarify details which have been suppressed in this concise description. We conclude this section by discussing some general features of this approach.

1.4. Comments on the algorithm

1.4.1. Level truncation

Because the matrices involved in these diagrams are infinite, it is difficult to analytically evaluate the integrals in (1.16), even for simple diagrams. It is easy, however, to truncate these matrices at a finite oscillator level, giving an expression which can be computed and numerically integrated, even up to high oscillator levels. From the point of view of the open string, this truncation essentially amounts to imposing a UV cutoff on string theory. This regularization breaks many of the desirable features of string theory, such as the large gauge symmetry and duality symmetries. Nonetheless, as we will describe in the following section, this truncation allows us to accurately approximate many on-shell and off-shell quantities of interest.

1.4.2. Equivalent formulations

Instead of placing all the vertices on the right in (1.11), we could put some vertices on the left and some on the right. An example of such a calculation is mentioned below in connection with (2.6). While the resulting expressions cannot be written as easily for a general diagram, this is often a convenient trick to simplify the evaluation of some particular amplitude at a fixed level of truncation. For tree-level diagrams, it is always possible to place half the vertices on the left and the other half on the right, leading to a reduction in the size of the matrices by a factor of 2. A similar procedure is possible for loop diagrams, although each fundamental loop with an odd number of vertices requires an additional block in the matrices.

1.4.3. Analytic evaluation

We do not yet have tools adequate to perform a direct analytic evaluation of any string amplitudes constructed in this fashion. Recent work [23] on the diagonalization of the Neumann coefficient matrices N^{rs}, however, gives hope that progress may be possible towards an analytic understanding of the determinants involved in (1.16). In particular, it would be interesting to ascertain whether a similar diagonalization could be carried out for the Neumann coefficient matrices after factors of $e^{-nT_r/2}$ are multiplied into the matrices on each side. Results in this direction might lead to new methods for analytically computing on-shell and off-shell string amplitudes.

2. Examples

In this section we present several examples of the algorithm described in Section 1.3.

2.1. Tree-level 4-tachyon amplitude at $p = 0$

For a first simple example, consider the off-shell tree-level 4-point function of the tachyon, where all external edges are taken to have momentum $p = 0$. The relevant diagram is depicted in Figure 1, where all incoming momenta are taken to vanish. Because our external states are all tachyons, we can drop all oscillators associated with external edges, and we only need to concern ourselves with the oscillators associated with the two halves of the single internal edge. Since all momenta vanish, we can drop all momenta from the calculation.

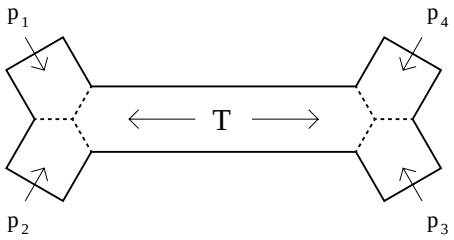

Figure 1: Tree-level 4-point function

For this diagram, the permutation matrix S connecting the half-edges is given by

$$S = \begin{pmatrix} 0 & C \\ C & 0 \end{pmatrix} . \tag{2.1}$$

The matrix $\tilde{N}$ can be written in terms of 2×2 infinite blocks as

$$\tilde{N}(T) = \begin{pmatrix} \hat{N}^{11}_{nm}(e^{-T}, e^{-T}) & 0 \\ 0 & \hat{N}^{11}_{nm}(e^{-T}, e^{-T}) \end{pmatrix} , \tag{2.2}$$

where

$$\hat{N}^{11}_{nm}(x, y) = x^{n/2} N^{11}_{nm} y^{m/2} . \tag{2.3}$$

Similarly, we have

$$\tilde{X}(T) = \begin{pmatrix} \hat{X}^{11}_{nm}(e^{-T}, e^{-T}) & 0 \\ 0 & \hat{X}^{11}_{nm}(e^{-T}, e^{-T}) \end{pmatrix} . \tag{2.4}$$

The off-shell $p = 0$ tree-level 4-tachyon amplitude is then given by

$$\mathcal{A}_4 = \int_0^\infty dT \, e^T \, \frac{\det(1 + S\tilde{X}(T))}{\det(1 - S\tilde{N}(T))^{13}} . \tag{2.5}$$

Note that this amplitude can also be written

$$\mathcal{A}_4 = \int_0^1 \frac{dx}{x^2} \frac{\det\left(1 - [C\hat{X}^{11}(x,x)]^2\right)}{\det\left(1 - [C\hat{N}^{11}(x,x)]^2\right)}. \tag{2.6}$$

This form of the amplitude can be derived from (2.5), or can be constructed directly by modifying the general algorithm so that one vertex is included on the left in (1.11) and the other on the right, as mentioned in 1.4.2. This form of the amplitude is useful because it involves smaller matrices which are easier to compute in level truncation.

If we remove by hand from the amplitude (2.5) the contribution coming from the intermediate tachyon state, we get the coefficient c_4 of ϕ^4 in the effective action for the $p = 0$ tachyon field ϕ when all other string fields are integrated out. An integral expression for this coefficient was given in [24], and evaluated numerically to an accuracy of 1%, giving $c_4 \approx -1.75 \pm 0.02$. We have repeated this calculation to a higher degree of precision, with the result

$$c_4 \approx -1.742 \pm 0.001\,. \tag{2.7}$$

The coefficient c_4 was computed using level truncation including all intermediate fields up to level 4 in [6] and including fields up to level 20 in [15]. The level 20 approximation gives $c_4^{[20]} = -1.684$, within 5% of the exact result.

Including the numerical factors associated with the symmetry of the diagram in Figure 1, we have

$$c_4 = \frac{9}{2} \int_0^\infty dT\; e^T \left[\frac{\det(1 + S\tilde{X}(T))}{\det(1 - S\tilde{N}(T))^{13}} - 1 \right]. \tag{2.8}$$

It is instructive to see how the level truncation in oscillator level works as a systematic approximation scheme for (2.8). The simplest level truncation involves dropping all oscillators other than a_1, a_{-1}. We then have the finite-size matrices

$$S = \begin{pmatrix} 0 & -1 \\ -1 & 0 \end{pmatrix}, \tag{2.9}$$

$$\tilde{N}(T) = \begin{pmatrix} \frac{5}{27} e^{-T} & 0 \\ 0 & \frac{5}{27} e^{-T} \end{pmatrix}, \tag{2.10}$$

$$\tilde{X}(T) = \begin{pmatrix} -\frac{11}{27} e^{-T} & 0 \\ 0 & -\frac{11}{27} e^{-T} \end{pmatrix}, \tag{2.11}$$

where we have used $N_{11}^{11} = 5/27, X_{11}^{11} = -11/27$ (note again that the sign convention used here is opposite to that used in [15]). Evaluating the determinants and replacing $x = e^{-T}$ gives

$$c_4^{(1)} = -\frac{9}{2} \int_0^1 \frac{dx}{x^2} \left[\frac{1 - \frac{121}{729} x^2}{(1 - \frac{25}{729} x^2)^{13}} - 1 \right]. \tag{2.12}$$

This approximation to c_4 includes contributions from an infinite number of intermediate fields—namely, all fields associated with states produced by acting with $b_{-1}c_{-1}$ and $(a_{-1}\cdot a_{-1})^k$ on the ground state. Performing a power series expansion in x, we have

$$c_4 \approx -\frac{9}{2}\int_0^1 dx\ \left[\frac{68}{243}+\frac{650}{19683}x^2+\cdots\right]. \tag{2.13}$$

Including only the first term, we have

$$c_4 \approx -\frac{34}{27} \approx -1.26\,. \tag{2.14}$$

This term represents all contributions from intermediate states at level 2; all such states can be constructed using oscillators of mode number 1. This number agrees with the calculation using level truncation on the level of intermediate states in [6, 15]. Including the second term in (2.13) shifts c_4 to ≈ -1.30879. This shift arises from the intermediate fields associated with the states $(a_{-1}\cdot a_{-1})^2|0\rangle$ and $(a_{-1}\cdot a_{-1})b_{-1}c_{-1}|0\rangle$, and again agrees with previous calculations. Integrating (2.12) gives

$$c_4^{(1)} = -\frac{5400229382637192721046565928004 85}{6736731352324653946302329289441 28}+\frac{14196819}{10485760}\ln\frac{11}{16} \approx -1.30891\,. \tag{2.15}$$

This shows that the contribution to c_4 from high level fields composed completely of level 1 oscillators is quite small.

We can get successfully better approximations to (2.8) by truncating (2.2, 2.4) at higher oscillator level L. Because this calculation simply involves numerically integrating a determinant of a symmetric $L\times L$ matrix, this calculation is significantly more efficient than using level truncation on states and separately summing over all intermediate states in the diagram, as done in [6, 15]. Numerical results for the approximation $c_4^{(L)}$ truncated at oscillator level $L \le 100$ are shown in Figure 2. At level 100, we have $c_4^{(100)} = -1.734$, within 1% of the value (2.7). Studying the large L behavior of $c_4^{(L)}$ suggests that the error introduced by truncating at level L decreases with a leading term of order $1/L$. A least-squares fit for the last 50 terms gives

$$c_4^{(L)} \approx -1.742 + \frac{0.80}{L} + \cdots \tag{2.16}$$

in complete agreement with (2.7). It would be interesting to find an analytic proof that contributions including oscillators at level L (and no higher-level oscillators) decrease at the rate L^{-2}.

It is interesting to see how the integrand in (2.8) approaches its exact form as $L \to \infty$. Analytic formulae for this integrand were calculated by Sloan [12] and by Samuel [13], following Giddings' analysis of the on-shell Veneziano amplitude [11] using the conformal mapping approach. We summarize some of this work in the Appendix, where Samuel's analytic formula for the integrand is related to the integrand of (2.5) through the relation (A.12). In Figure 3, we have graphed the integrand (without the subtraction of the divergent tachyon term) at various cutoff levels L and compared to the exact formula (A.12). The

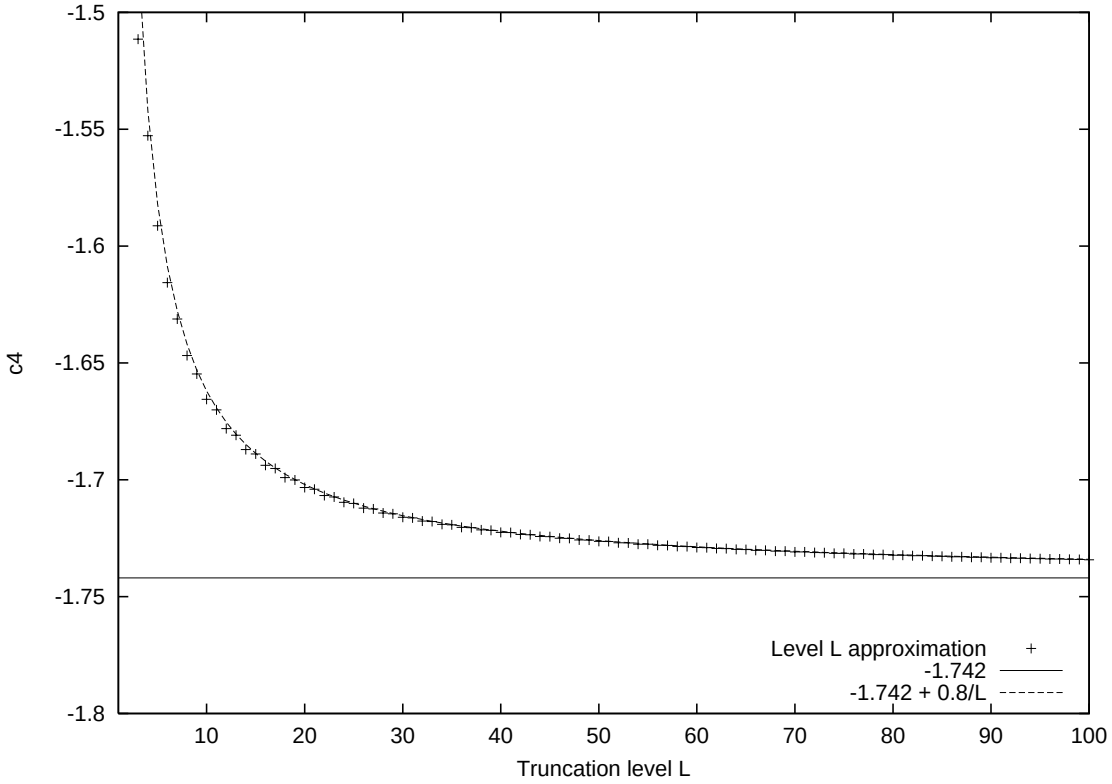

Figure 2: Level-truncated approximations to c_4

integrand converges very rapidly (apparently exponentially rapidly) except near $x = 1$. This rapid convergence away from $x = 1$ is natural, as the cutoff at level L gets all terms in a power series expansion of the integrand in x correct up to order x^{L+1}. The parameter x goes to 1 when the length of the intermediate propagator goes to 0, so that level truncation here is playing the role of a UV cutoff.

2.2. Tree-level 4-tachyon amplitude ($p_i \neq 0$)

Now let us consider the tachyon 4-point function with arbitrary external momenta. The on-shell tachyon 4-point function was computed from string field theory in [11] using the conformal mapping method, and shown to agree with the Veneziano amplitude. Later, the off-shell tachyon 4-point function was computed using similar methods in [12, 13]. An expression for the amplitude in terms of infinite matrices was also derived in [13] using the oscillator approach, but it was not shown that this expression agreed with the analytic formula arising from the conformal mapping approach. In this subsection we summarize the results of using our algorithm to directly compute the Veneziano amplitude and its off-shell generalization. The relationship between these results and those of [11, 12, 13] are discussed in the Appendix.

In the 4-point tachyon diagram shown in Figure 1, momentum conservation ensures

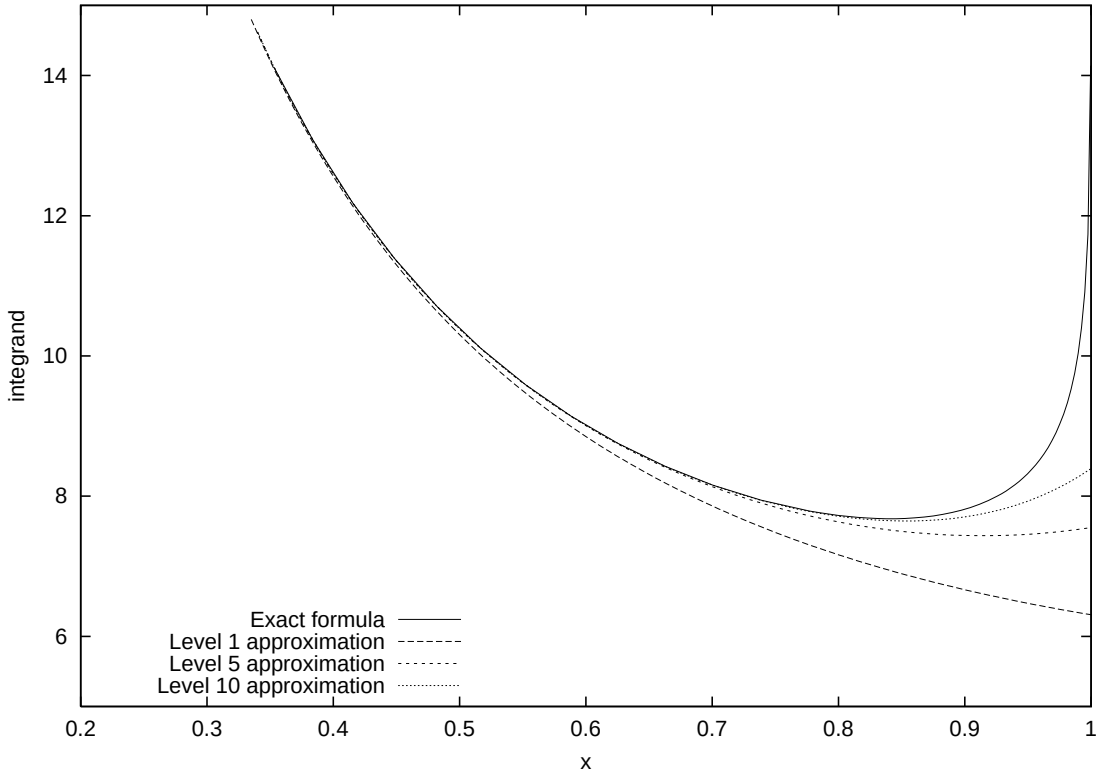

Figure 3: Momentum-independent 4-tachyon integrand

$p_1 + p_2 + p_3 + p_4 = 0$. The on-shell Veneziano amplitude associated with this diagram is (setting $\alpha' = 1$)

$$\mathcal{A}_4^{[V]}(p_1, p_2, p_3, p_4) = B(-s-1, -t-1) \tag{2.17}$$

where $B(u, v)$ is the Euler beta function, and s, t are the Mandelstam variables

$$s = -(p_1 + p_2)^2, \qquad t = -(p_2 + p_3)^2, \tag{2.18}$$

The Euler beta function has the integral representation

$$B(u, v) = \int_0^1 d\xi \; \xi^{u-1}(1-\xi)^{v-1} \,. \tag{2.19}$$

This integral representation of the Veneziano amplitude is convergent when $u, v > 0$, so that $s, t < -1$. For positive real s, t it is necessary to perform an analytic continuation to make sense of (2.19) away from the poles at positive integers. The discovery of the Veneziano amplitude (2.17) marked the beginning of string theory [25]. We will now show how this amplitude can be reproduced numerically from string field theory using our general approach to amplitude calculation.

The 4-point tachyon amplitude with arbitrary external momenta takes the general form (1.16), where contraction with external tachyon states means that all oscillators $a^\dagger, b^\dagger, c^\dagger$ in the exponent can be dropped. The momentum-independent part of the integrand in this case

is identical to that of (2.5), which is just the general amplitude with all momenta vanishing. The momentum terms appearing in the initial amplitude (1.11), before removing internal oscillators, are given by

$$\exp\left(-\frac{1}{2}N_{00}^{11}[p_1^2+p_2^2+p_3^2+p_4^2+2(p_1+p_2)^2]\right)\ \times \qquad (2.20)$$
$$\exp\left(-T(p_1+p_2)^2\right)\exp\left(-p_iD_n^{ij}a_{-n}^{(j)}\right)$$

where

$$D_n=\begin{pmatrix} \hat{N}_{0n}^{12}(1,x)-\hat{N}_{0n}^{22}(1,x) & 0 \\ \hat{N}_{0n}^{32}(1,x)-\hat{N}_{0n}^{22}(1,x) & 0 \\ 0 & \hat{N}_{0n}^{23}(1,x)-\hat{N}_{0n}^{33}(1,x) \\ 0 & \hat{N}_{0n}^{13}(1,x)-\hat{N}_{0n}^{33}(1,x) \end{pmatrix} \qquad (2.21)$$

After contracting internal oscillators, this gives us a total amplitude

$$\mathcal{A}_4(p_1,p_2,p_3,p_4)=I(s,t)+I(t,s) \qquad (2.22)$$

where

$$I(s,t)=\frac{3^9}{2^{12}}\int_0^\infty dT\ e^T\ \frac{\det(1+S\tilde{X}(T))}{\det(1-S\tilde{N}(T))^{13}}\exp\left(-\frac{1}{2}p_iQ_{ij}p_j\right) \qquad (2.23)$$

with

$$Q_{ij}=N_{00}^{11}\begin{pmatrix}2&1&0&0\\1&2&0&0\\0&0&2&1\\0&0&1&2\end{pmatrix}+T\begin{pmatrix}1&1&0&0\\1&1&0&0\\0&0&1&1\\0&0&1&1\end{pmatrix}+D\frac{1}{1-S\tilde{N}}SD^T\,. \qquad (2.24)$$

Equations (2.23, 2.24) give a complete description of the off-shell generalization of the Veneziano amplitude (2.17). We have included in (2.23) the constant factor needed for agreement with (2.17). The two terms in (2.22) come from integration over the regions $\xi<1/2$, $\xi>1/2$, as discussed in the Appendix.

Let us now consider the level truncation approximations of (2.23, 2.24). At level 1, the matrices $S,\tilde{N},\tilde{X}$ in the integrand of (2.23) are given by (2.9-2.11). Using the values $N_{00}^{11}=\ln(27/16)$, $N_{01}^{12}=-N_{01}^{21}=2\sqrt{2}/3\sqrt{3}$, and their cyclic relatives, we have

$$Q_{ij}^{(1)}=\begin{pmatrix} \ln\frac{3^6}{2^8x}+\frac{40x^2}{729-25x^2} & \ln\frac{3^3}{2^4x}-\frac{40x^2}{729-25x^2} & -\frac{216x^2}{729-25x^2} & \frac{216x^2}{729-25x^2} \\ \ln\frac{3^3}{2^4x}-\frac{40x^2}{729-25x^2} & \ln\frac{3^6}{2^8x}+\frac{40x^2}{729-25x^2} & \frac{216x^2}{729-25x^2} & -\frac{216x^2}{729-25x^2} \\ -\frac{216x^2}{729-25x^2} & \frac{216x^2}{729-25x^2} & \ln\frac{3^6}{2^8x}+\frac{40x^2}{729-25x^2} & \ln\frac{3^3}{2^4x}-\frac{40x^2}{729-25x^2} \\ \frac{216x^2}{729-25x^2} & -\frac{216x^2}{729-25x^2} & \ln\frac{3^3}{2^4x}-\frac{40x^2}{729-25x^2} & \ln\frac{3^6}{2^8x}+\frac{40x^2}{729-25x^2} \end{pmatrix} \qquad (2.25)$$

The level 1 approximation to (2.23) is thus given by

$$\mathcal{A}_4^{(1)}(p_1,p_2,p_3,p_4)=I^{(1)}(s,t)+I^{(1)}(t,s) \qquad (2.26)$$

where

$$I(s,t)=\frac{3^9}{2^{12}}\int_0^1\frac{dx}{x^2}\ \frac{1-\frac{121}{729}x^2}{(1-\frac{25}{729}x^2)^{13}}\ \exp\left(-\frac{1}{2}p_iQ_{ij}^{(1)}p_j\right)\,. \qquad (2.27)$$

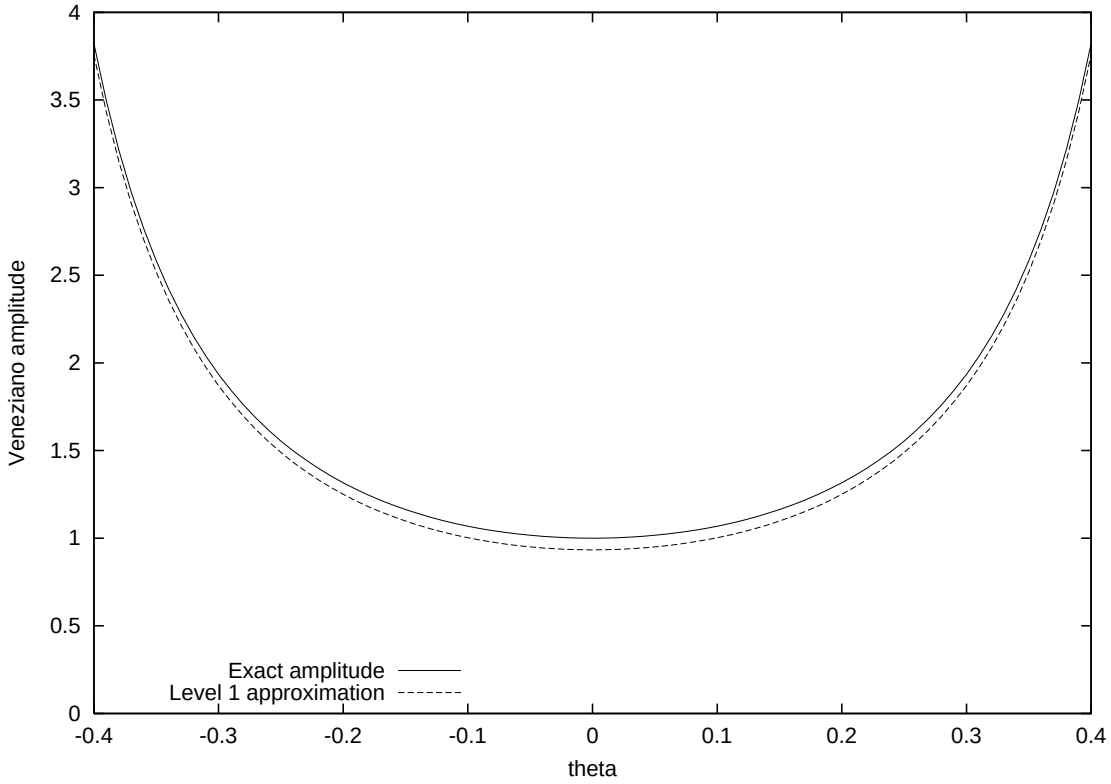

Figure 4: Veneziano amplitude at $s = -2 - 2\sin\theta, t = -2 + 2\sin\theta$

While the integral in (2.26) and the analogous integrals at higher levels of truncation are not analytically tractable, such integrals can be readily approximated numerically or by truncating a power series expansion for the integrand. To see how accurate the approximation (2.26) is, we can numerically compute the integral and compare to the Veneziano amplitude for particular values of the momenta. Let us consider in particular the case where $u = -(p_1 + p_3)^2 = 0$. In this case, when all particles are on-shell tachyons we have $s + t = -4$. We expect to have a convergent integral when $-3 < s, t < -1$. In this regime we can choose momenta

$$p_1 = (0, 1, 0, 0, \ldots, 0) \qquad p_2 = (0, \sin\theta, \cos\theta, 0, \ldots, 0) \tag{2.28}$$

$$p_3 = (0, -1, 0, 0, \ldots, 0) \qquad p_4 = (0, -\sin\theta, -\cos\theta, 0, \ldots, 0) \tag{2.29}$$

parameterized by θ, so that

$$s = -2 - 2\sin\theta, \qquad t = -2 + 2\sin\theta\,. \tag{2.30}$$

We expect to have a convergent expression for the amplitude when $-\pi/6 < \theta < \pi/6 \approx 0.5236$. In Figure 4 we have graphed the Veneziano amplitude in the range $|\theta| \leq 0.4$, and we have plotted the numerical values for the level 1 approximation (2.26).

The level 1 approximation to the Veneziano amplitude shown in Figure 4 is within 10% of the correct result at $\theta = 0$, and within 5% of the correct result at $\theta = 0.4$. In Figure 5 we

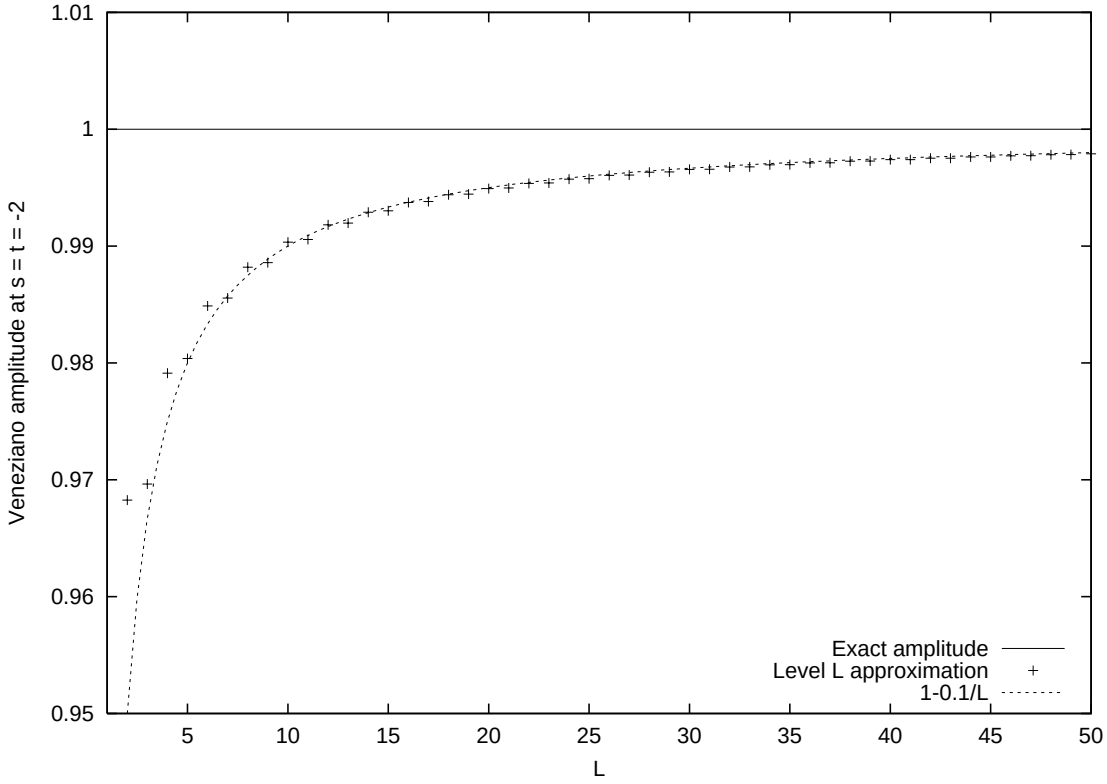

Figure 5: Veneziano amplitude at $s = t = -2$

have graphed the successive approximations to Veneziano at $\theta = 0$ ($s = t = -2$), up to level $L = 50$. At $\theta = 0$ the exact Veneziano amplitude is $B(1, 1) = 1$. The approximation at level 50 is

$$\mathcal{A}^{(50)}(s = t = -2) = 0.9979 \tag{2.31}$$

within about 0.2% of the exact answer. Just as for the coefficient c_4, it seems that the successive level approximations have errors which decrease as $1/L$. A least-squares fit for the last 25 terms gives

$$\mathcal{A}^{(L)}(s = t = -2) \approx 0.99993 - 0.10/L \tag{2.32}$$

Although the particular values of p_i for which we have computed here the approximation to Veneziano are on-shell, the same analysis can be done for off-shell amplitudes. The discussion in the previous subsection amounts to doing this in the case $p_i = 0$. We have found that in both the on-shell and off-shell cases the numerical approximations to the amplitudes given by truncation on oscillator mode level converge in a similar fashion, although the constant controlling the size of the error is smaller for the on-shell calculation.

We have explicitly described here the 4-point function for external tachyon states. This could be generalized in a straightforward fashion to include arbitrary external states by including the oscillators $a^{(i)}$ on the external edges. In Section 2.4 we do such a calculation for the one-loop one-point function, which has only one external string.

2.3. Tree-level N-point function

It is easy to generalize the discussion of the previous subsection to tree-level N-point functions, although as N increases the details become more complicated. We work out one further example here at tree level, that of the 5-tachyon amplitude at $p = 0$.

5-point function for 0-momentum tachyon

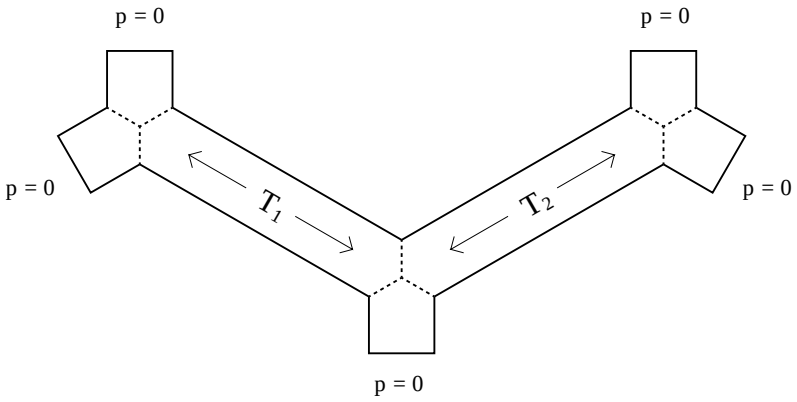

Figure 6: Tree-level $p = 0$ 5-tachyon amplitude

The 5-point function for the tachyon at $p = 0$ comes from the diagram in Figure 6. This amplitude is given by

$$\mathcal{A}_5 = \int \frac{dx}{x^2}\frac{dy}{y^2}\ \frac{\det(1 + S\tilde{X})}{\det(1 - S\tilde{N})^{13}} \tag{2.33}$$

where

$$x = e^{-T_1}, \qquad y = e^{-T_2}, \tag{2.34}$$

$$S = \begin{pmatrix} 0 & C & 0 & 0 \\ C & 0 & 0 & 0 \\ 0 & 0 & 0 & C \\ 0 & 0 & C & 0 \end{pmatrix}, \tag{2.35}$$

$$\tilde{N} = \begin{pmatrix} \hat{N}^{11}(x,x) & 0 & 0 & 0 \\ 0 & \hat{N}^{22}(x,x) & \hat{N}^{23}(x,y) & 0 \\ 0 & \hat{N}^{32}(y,x) & \hat{N}^{33}(y,y) & 0 \\ 0 & 0 & 0 & \hat{N}^{11}(y,y) \end{pmatrix}, \tag{2.36}$$

and an identical expression to (2.36) gives $\tilde{X}$, where all appearances of $\hat{N}$ are replaced by $\hat{X}$. Writing the integrand in (2.33) as $F(x, y)$, the coefficient c_5 in the tachyon effective potential is given by

$$c_5 = 27 \int \frac{dx}{x^2}\frac{dy}{y^2}\ \left[F(x,y) - F(x,0) - F(0,y) + F(0,0)\right], \tag{2.37}$$

where the subtractions have the effect of removing the terms associated with intermediate open string tachyon states.

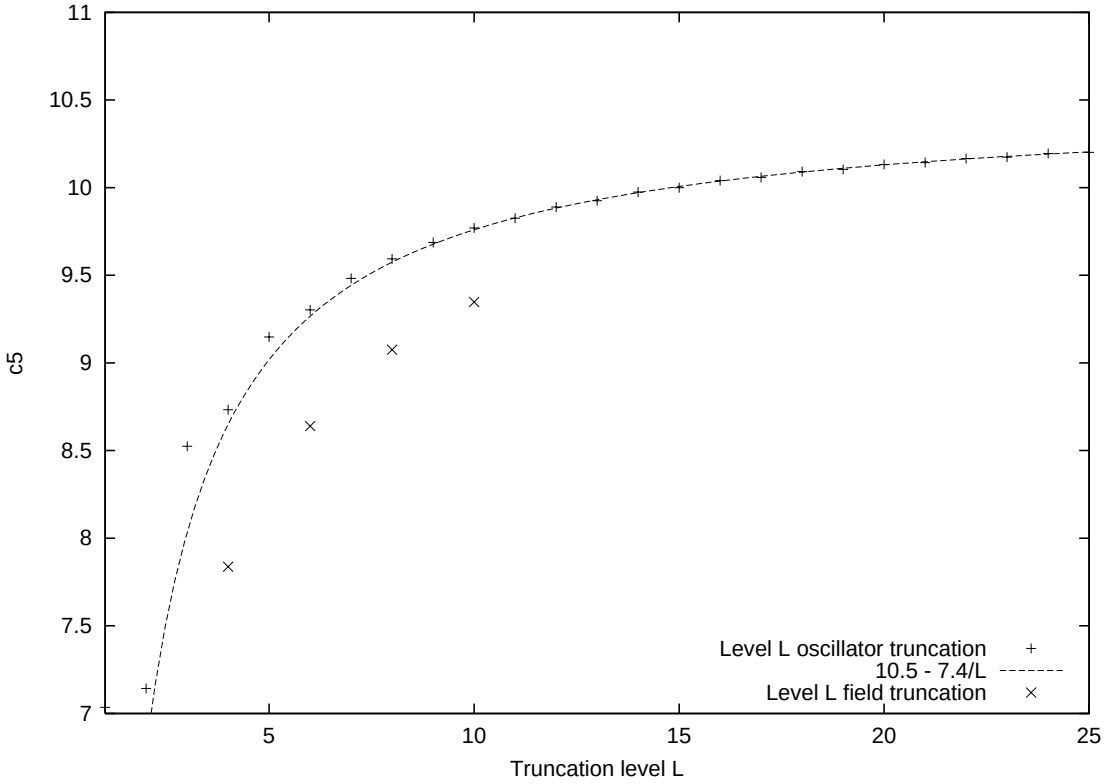

Figure 7: Approximations to c_5

No exact expression is known for the coefficient c_5. Approximate values of c_5 were computed in [8] using level truncation on fields, up to level 10. At level 10, we found $c_5^{[10]} = 9.35$. Approximations computed using (2.37) are graphed in Figure 7 using oscillators up to level 25. The results of [8] using level truncation on fields are included for comparison. At level 25 we have $c_5^{(25)} = 10.20$. Although we have less data in this case, it seems that again the error goes as $1/L$. A least-squares fit on the last 10 data points gives

$$c_5^{(L)} \approx 10.5 - 7.4/L\,. \tag{2.38}$$

2.4. One-loop 1-point function

Consider now the one-loop one-point function shown in Figure 8. By momentum conservation the external momentum is 0, while we must integrate over the internal momentum q. In this example we will include all external oscillators, so that this one-point function will be a state $|\mathcal{S}\rangle$ in the Fock space. To compute the tadpole for any particular field, the appropriate state should be contracted with $|\mathcal{S}\rangle$.

Using the general formalism described in 1.3, we have

$$|\mathcal{S}\rangle = \int_0^1 \frac{dx}{x^2} \int d^{26}q\, \frac{\det(1+S\tilde{X})}{\det(1-S\tilde{N})^{13}} \tag{2.39}$$

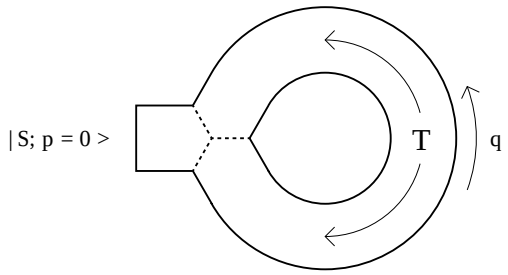

Figure 8: One-loop one-point diagram

$$\times \exp\left(-\frac{1}{2}a_{-n}Q_{nm}a_{-m} - a_{-n}Q_n q - \frac{1}{2}q^2 Q - c_{-n}R_{nm}b_{-m}\right)|0;0\rangle$$

where

$$S = \begin{pmatrix} 0 & C \\ C & 0 \end{pmatrix}, \qquad \tilde{N} = \begin{pmatrix} \hat{N}^{22}(x,x) & \hat{N}^{23}(x,x) \\ \hat{N}^{32}(x,x) & \hat{N}^{33}(x,x) \end{pmatrix}, \qquad \tilde{X} = \begin{pmatrix} \hat{X}^{22}(x,x) & \hat{X}^{23}(x,x) \\ \hat{X}^{32}(x,x) & \hat{X}^{33}(x,x) \end{pmatrix} \tag{2.40}$$

and

$$\begin{aligned}
Q_{nm} &= N^{11}_{nm} + \begin{pmatrix} \hat{N}^{12}_{n\cdot}(1,x) \\ \hat{N}^{13}_{n\cdot}(1,x) \end{pmatrix}^T \frac{1}{1-S\tilde{N}} S \begin{pmatrix} \hat{N}^{21}_{\cdot m}(x,1) \\ \hat{N}^{31}_{\cdot m}(x,1) \end{pmatrix} \\
Q_n &= N^{12}_{n0} - N^{13}_{n0} + \begin{pmatrix} \hat{N}^{12}_{n\cdot}(1,x) \\ \hat{N}^{13}_{n\cdot}(1,x) \end{pmatrix}^T \frac{1}{1-S\tilde{N}} S \begin{pmatrix} \hat{N}^{22}_{\cdot 0}(x,1) - \hat{N}^{23}_{\cdot 0}(x,1) \\ \hat{N}^{32}_{\cdot 0}(x,1) - \hat{N}^{33}_{\cdot 0}(x,1) \end{pmatrix} \\
Q &= N^{11}_{00} + \begin{pmatrix} \hat{N}^{22}_{0\cdot}(1,x) - \hat{N}^{32}_{0\cdot}(1,x) \\ \hat{N}^{23}_{0\cdot}(1,x) - \hat{N}^{33}_{0\cdot}(1,x) \end{pmatrix}^T \frac{1}{1-S\tilde{N}} S \begin{pmatrix} \hat{N}^{22}_{\cdot 0}(x,1) - \hat{N}^{23}_{\cdot 0}(x,1) \\ \hat{N}^{32}_{\cdot 0}(x,1) - \hat{N}^{33}_{\cdot 0}(x,1) \end{pmatrix} \\
R_{nm} &= X^{11}_{nm} + \begin{pmatrix} \hat{X}^{12}_{n\cdot}(1,x) \\ \hat{X}^{13}_{n\cdot}(1,x) \end{pmatrix}^T \frac{1}{1-S\tilde{X}} S \begin{pmatrix} \hat{X}^{21}_{\cdot m}(x,1) \\ \hat{X}^{31}_{\cdot m}(x,1) \end{pmatrix}
\end{aligned} \tag{2.41}$$

Integrating (2.39) over the internal momentum q gives (up to a constant)

$$|\mathcal{S}\rangle = \int_0^1 \frac{dx}{x^2} \, \frac{\det(1+S\tilde{X})}{\det(1-S\tilde{N})^{13} Q^{13}} \exp\left(-\frac{1}{2}a_{-n}\left(Q_{nm} - \frac{Q_n Q_m}{Q}\right)a_{-m} - c_{-n}R_{nm}b_{-m}\right)|0;0\rangle \tag{2.42}$$

This diagram represents a tadpole in the D25-brane background. A thorough analysis of this diagram should give a number of interesting results. We restrict ourselves here to some brief comments on this subject, however. Just as for the tree-level 4-point amplitude discussed above, the integrand in (2.42) converges rapidly for $x < 1$ in the oscillator level-truncation approximation. The integrand has singularities at $x = 0$ and $x = 1$, corresponding to the closed and open string tachyons. At $x = 1$, the quadratic term in the exponential has a limit where $R_{nm} = C_{nm}$, with a similar result for the matter fields. This form of squeezed state was identified by Shapiro and Thorn as being an open string representation

of a closed string state [26]. With a more careful analysis it should be possible to show that this diagram gives rise to precisely the closed string tadpoles expected from the bosonic disk diagram with a single closed string vertex operator at a point in the interior. This result would demonstrate that when quantum effects are included, the open string field is naturally pushed in a direction associated with turning on closed string degrees of freedom, without having to introduce the closed strings by hand.

Related issues to those just mentioned arise when one considers the one-loop nonplanar 2-point function, which has a similar expression to (2.42). This amplitude was computed in string field theory using the conformal mapping method by Freedman, Giddings, Shapiro and Thorn [14], who showed that the closed string poles naturally appear in this amplitude and are associated with states of the Shapiro-Thorn form mentioned above. It would be very satisfying to see how this result arises from the formalism of this paper. Further study of one-loop amplitudes in the open bosonic string using these methods is left to future work.

2.5. Higher loops

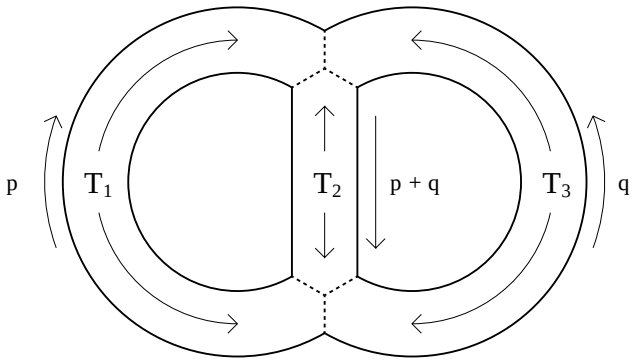

Figure 9: Two-loop vacuum graph

It is clear that the methods we have developed here can be generalized to diagrams with an arbitrary number of internal loops. As a final example, let us consider the simplest 2-loop diagram, Figure 9, giving a contribution to the vacuum energy. This diagram gives a contribution of

$$\mathcal{F}_{2-\text{loop}} = \int \frac{dx}{x^2}\frac{dy}{y^2}\frac{dz}{z^2}\; d^{26}p\, d^{26}q\; \frac{\det(1+S\tilde{X})}{\det(1-S\tilde{N})^{13}} \exp\left(-\frac{1}{2}\,(q\;p)\,Q\begin{pmatrix} q \\ p \end{pmatrix}\right) \tag{2.43}$$

where

$$x = e^{-T_1}, \qquad y = e^{-T_2}, \qquad z = e^{-T_3}, \tag{2.44}$$

$$S = \begin{pmatrix} 0 & 0 & 0 & C & 0 & 0 \\ 0 & 0 & 0 & 0 & 0 & C \\ 0 & 0 & 0 & 0 & C & 0 \\ C & 0 & 0 & 0 & 0 & 0 \\ 0 & 0 & C & 0 & 0 & 0 \\ 0 & C & 0 & 0 & 0 & 0 \end{pmatrix}, \tag{2.45}$$

$$\tilde{N} = \begin{pmatrix} \hat{N}^{11}(x,x) & \hat{N}^{12}(x,z) & \hat{N}^{13}(x,y) & 0 & 0 & 0 \\ \hat{N}^{21}(z,x) & \hat{N}^{22}(z,z) & \hat{N}^{23}(z,y) & 0 & 0 & 0 \\ \hat{N}^{31}(y,x) & \hat{N}^{32}(y,z) & \hat{N}^{33}(y,y) & 0 & 0 & 0 \\ 0 & 0 & 0 & \hat{N}^{11}(x,x) & \hat{N}^{12}(x,y) & \hat{N}^{13}(x,z) \\ 0 & 0 & 0 & \hat{N}^{21}(y,x) & \hat{N}^{22}(y,y) & \hat{N}^{23}(y,z) \\ 0 & 0 & 0 & \hat{N}^{31}(z,x) & \hat{N}^{32}(z,y) & \hat{N}^{33}(z,z) \end{pmatrix}, \tag{2.46}$$

and where $\tilde{X}$ is given by an identical expression to (2.46), but with $\hat{N}$ replaced by $\hat{X}$. The momentum matrix Q from (2.43) is given by

$$Q = 4N_{00}^{11} \begin{pmatrix} 1 & 1 \\ 1 & 1 \end{pmatrix} + \begin{pmatrix} 2T_2 + 2T_3 & T_2 \\ T_2 & 2T_1 + 2T_2 \end{pmatrix} + D^T \frac{1}{1 - S\tilde{N}} SD \tag{2.47}$$

where

$$D = \begin{pmatrix} -\hat{N}^{12}_{n0}(x,1) + \hat{N}^{13}_{n0}(x,1) & \hat{N}^{11}_{n0}(x,1) - \hat{N}^{13}_{n0}(x,1) \\ -\hat{N}^{22}_{n0}(z,1) + \hat{N}^{23}_{n0}(z,1) & \hat{N}^{21}_{n0}(z,1) - \hat{N}^{23}_{n0}(z,1) \\ -\hat{N}^{32}_{n0}(y,1) + \hat{N}^{33}_{n0}(y,1) & \hat{N}^{31}_{n0}(y,1) - \hat{N}^{33}_{n0}(y,1) \\ \hat{N}^{12}_{n0}(x,1) - \hat{N}^{13}_{n0}(x,1) & -\hat{N}^{11}_{n0}(x,1) + \hat{N}^{13}_{n0}(x,1) \\ \hat{N}^{22}_{n0}(y,1) - \hat{N}^{23}_{n0}(y,1) & -\hat{N}^{21}_{n0}(y,1) + \hat{N}^{23}_{n0}(y,1) \\ \hat{N}^{32}_{n0}(z,1) - \hat{N}^{33}_{n0}(z,1) & -\hat{N}^{31}_{n0}(z,1) + \hat{N}^{33}_{n0}(z,1) \end{pmatrix}. \tag{2.48}$$

Integrating over p, q gives

$$\mathcal{F}_{2-\text{loop}} = \int \frac{dx}{x^2} \frac{dy}{y^2} \frac{dz}{z^2} \, f(x,y,z), \tag{2.49}$$

where

$$f(x,y,z) = \frac{\det(1 + S\tilde{X})}{[\det(1 - S\tilde{N}) \det Q]^{13}} \tag{2.50}$$

This gives the 2-loop contribution to the vacuum energy of open string field theory in the standard vacuum containing a D25-brane. This expression contains divergences, such as that arising from the closed string tachyon when the parameters x, y and z go to 1, so the integral is not finite. At generic values of the parameters, however, the integrand is finite. A level-truncation analysis of the integrand at fixed values of x, y, z, such as at $x = y = z = 1/2$, indicates that the value of the integrand converges exponentially rapidly as higher level oscillators are included, just as for the integrand of the four-point tree amplitude and the one-point one-loop amplitude described above. Further study of loop amplitudes is left to future work. It would be particularly interesting to study the convergence properties of the integrand for nonplanar diagrams at higher genus.

3. Discussion

In this paper we have presented a simple algorithm which gives a closed-form expression for any open string amplitude at any loop order, using string field theory. For any diagram, the resulting amplitude is an integral over a finite number of well-defined modular parameters of a function of some infinite-dimensional matrices built from a finite number of blocks containing the Witten 3-string vertex. Using level truncation on oscillator level, this gives an algorithm for systematically computing any open string amplitude to an arbitrary degree of accuracy. We find that for both tree and loop diagrams, the integrand of the amplitude converges very rapidly under level truncation, although the rate of convergence becomes slower as the Witten parameter T associated with the length of an internal edge of a diagram goes to 0. For all finite tree amplitudes we considered, we found that the error introduced by a truncation at oscillator level L goes as $1/L$.

There are many potentially interesting applications of this approach, and many ways in which it would be interesting to extend this work. We mention a few of these directions briefly here.

• We do not yet have sufficient analytic control of the infinite matrices appearing in the string field theory amplitudes to evaluate even the simplest diagrams exactly. It would be very interesting to generalize the recent work on the diagonalization of the matrices of Neumann coefficients for the Witten vertex [23] to the matrices $\hat{N}$ defined through (1.13). Such a generalization might lead naturally to exact analytic expressions for amplitudes, at least for simple diagrams.

• We find empirically that truncation at oscillator level L of the string field theory expression for the Veneziano amplitude and its off-shell generalization introduces an error of order $1/L$. We found the same kind of convergence for the off-shell $p = 0$ 5-tachyon amplitude. It would be interesting to prove this result rigorously for these amplitudes, and to understand the rate of convergence of this approximation for more complicated diagrams.

• While the analysis of this paper focuses on Witten's cubic open bosonic string field theory, the methods can be generalized to other string field theories. It would be particularly interesting to apply this method to superstring field theory, either in the Berkovits [27] or Witten [28, 29] formulation. Since there is currently no method available for explicitly computing covariant on-shell correlation functions of superstrings at high loop order/genus (see [30] for some recent work at two-loop order in closed strings), this method might lead to interesting new results for on-shell superstring amplitudes. This method can also be used as a means of checking the various proposals for superstring field theory. Since loop diagrams in superstring field theory do not have the divergence problems arising from tachyons which afflict loop diagrams in the bosonic theory, we expect that this approach may provide a useful means of numerically calculating high-order loop diagrams in superstring theory.

• A crucial question in open string field theory, which has been brought back to the fore

by recent developments related to Sen's tachyon condensation conjectures, is how closed strings are encoded in open string field theory, and whether closed strings can be treated as asymptotic on-shell states using only the degrees of freedom of open string field theory [31]. A careful study of open string loop amplitudes using the methods of this paper may lead to new insight into this question.

• Related to the closed string issue is that of what the natural degrees of freedom are which should describe open string field theory after the tachyon has condensed into the stable vacuum. In this vacuum there are no open string degrees of freedom [32, 33]. It would be very interesting if the methods of this paper could be generalized to study the vacuum string field theory (VSFT) in this stable vacuum, either directly through expanding around the nontrivial solution of the Witten theory as in [32, 33], or using the RSZ pure ghost Ansatz for the BRST operator [34]

• Finally, the methods described here might be used to compute the effective action for the gauge field and/or the tachyon on a system of multiple Dp-branes, along the lines of [15]. This might lead to new insight into the form of the resulting nonabelian Born-Infeld action and/or the tachyon effective field theory, neither of which are yet completely understood.

Acknowledgements

I would like to thank Erasmo Coletti, Ian Ellwood, Steve Giddings, Michael Green, Ashoke Sen, Jessie Shelton, Ilia Sigalov, and Barton Zwiebach for helpful discussions. I would also like to thank the Newton Institute and the organizers of the Newton Institute workshop on M-theory for support and hospitality while much of this work was done. The numerical computations described in this work were done using *Mathematica*. This work was supported by the DOE through contract #DE-FC02-94ER40818.

A. Analytic description of 4-tachyon amplitude

In this Appendix we briefly summarize the results of [11, 12, 13] which give an analytic description of the on-shell and off-shell 4-tachyon amplitude from string field theory.

In [11], Giddings gave an explicit conformal map which takes the Riemann surface defined by the Witten diagram with internal edge of length T to the standard disc with four tachyon vertex operators on the boundary, parameterized by the Koba-Nielsen parameter ξ (usually called x). This conformal map is defined in terms of four parameters $\alpha, \beta, \gamma, \delta$ satisfying the relations

$$\alpha\beta = \gamma\delta = 1 \tag{A.1}$$

and

$$\frac{1}{2} = \Lambda_0(\theta_1, k) - \Lambda_0(\theta_2, k) \tag{A.2}$$

where $\Lambda_0(\theta, k)$ is Heuman's lambda function, defined as

$$\Lambda_0(\theta, k) = \frac{2}{\pi}\left(E(k)F(\theta, k') + K(k)(E(\theta, k') - F(\theta, k'))\right) \tag{A.3}$$

in terms of the complete elliptic integrals of the first and second kinds $K(k), E(k)$ and the incomplete elliptic integral of the first kind $F(\theta, k)$, and the parameters $\theta_1, \theta_2, k, k'$ given by

$$k = \gamma^2 \qquad\qquad k' = \sqrt{1-k^2} \tag{A.4}$$

$$\theta_1 = \sin^{-1}\frac{\beta}{\sqrt{\beta^2+\gamma^2}} \qquad\qquad \theta_2 = \sin^{-1}\frac{\alpha}{\sqrt{\alpha^2+\gamma^2}}\,. \tag{A.5}$$

Since the four parameters $\alpha - \delta$ are related by the three relations (A.1, A.2), all the parameters can be considered as functions of α.

The Witten parameter T is related to the parameter α through

$$T = 2K(k')\left(Z(\theta_2, k') - Z(\theta_1, k')\right) \tag{A.6}$$

where $Z(\theta, k)$ is Jacobi's zeta function

$$Z(\theta, k) = E(\theta, k) - \frac{E(k)}{K(k)}F(\theta, k)\,. \tag{A.7}$$

The parameter α is in turn related to the Koba-Nielsen parameter ξ through

$$\alpha = \sqrt{\frac{1-\sqrt{\xi}}{1+\sqrt{\xi}}}\,. \tag{A.8}$$

When $T = 0$ we have $\alpha = -1 + \sqrt{2}$ and $\xi = 1/2$. When $T = \infty$ we have $\alpha = 0$ and $\xi = 1$. For $\xi < 1/2$, the associated Witten diagram is in the opposite (t) channel from that shown in Figure 1. This explains the two terms in (2.26).

In [11], Giddings used the conformal map just described to map the string field theory calculation of the on-shell 4-tachyon amplitude to a conformal field theory calculation, and showed that the result of the string field theory calculation is indeed the Veneziano amplitude. In [12, 13], Samuel and Sloan used Giddings' approach and with some additional analysis found an analytic formula for the off-shell 4-tachyon amplitude. The off-shell amplitude differs from the Veneziano amplitude in that it has an additional term in the integrand of (for $1/2 < \xi < 1$, using the notation of [13])

$$\left(\frac{\kappa(\xi)}{2}\right)^{p_1^2+p_2^2+p_3^2+p_4^2-4} \tag{A.9}$$

where

$$\kappa = \exp\left(-N\beta\int_1^\infty dw\ \ln(w-1)\frac{\mathrm{d}}{\mathrm{d}w}\left[\frac{\sqrt{(w^2+a^2\gamma^2)(w^2+\alpha^2\delta^2)}}{(w+1)(\beta^2w^2-\alpha^2)}\right]\right) \tag{A.10}$$

with

$$N = 2\alpha\frac{\beta^2-\alpha^2}{\sqrt{(\alpha^2+\gamma^2)(\alpha^2+\delta^2)}}\,. \tag{A.11}$$

It is clear that (A.9) vanishes on-shell, where $p_i^2 = 1$.

Relating the off-shell Veneziano integrand at $p = 0$ with the correction (A.9) to the integrand appearing in (2.23), the expressions agree if [13]

$$\frac{3^9}{2^{12}x}\frac{\det(1+S\tilde{X})}{\det(1-S\tilde{N})^{13}} = \frac{4}{\pi\kappa^4}\sqrt{(\alpha^2+\gamma^2)(\beta^2+\gamma^2)}(\beta^2-\alpha^2)K(\gamma^2)\,. \tag{A.12}$$

The extent to which these expressions agree at a finite level of truncation controls the rate of convergence of the level-truncated approximations to the on-shell and off-shell 4-point amplitudes, such as those discussed in Section 2.1 and 2.2. In Figure 3 we have graphed the RHS of (A.12) and compared with low-level truncations. As discussed in Section 2.1, the convergence is extremely fast except near $x = 1$.

The comparison just done relates the analytic formula for the momentum-independent part of the off-shell four-tachyon amplitude found in [12, 13] to the matrix expression calculated using the oscillator methods of this paper. It is also possible to relate the momentum-dependent factors. In [12, 13], explicit formulae were given for the momentum-dependent factors in the off-shell extension of the Veneziano integrand. These can be related to the matrices Q_{ij} of (2.24), although the comparison is not direct since the matrices are subject to a redefinition using the conservation law $\sum_i p_i = 0$. The computation of the on-shell Veneziano amplitude in Section 2.2 demonstrates that the momentum-dependent terms also agree on shell.

References

[1] E. Witten, "Non-commutative geometry and string field theory," Nucl. Phys. **B268** 253 (1986).

[2] A. Sen, "Universality of the tachyon potential," JHEP **9912**, 027 (1999), hep-th/9911116.

[3] K. Ohmori, "A review on tachyon condensation in open string field theories," hep-th/0102085.

[4] P. J. De Smet, "Tachyon condensation: Calculations in string field theory," hep-th/0109182.

[5] I. Y. Arefeva, D. M. Belov, A. A. Giryavets, A. S. Koshelev and P. B. Medvedev, "Noncommutative field theories and (super)string field theories," hep-th/0111208.

[6] V. A. Kostelecky and S. Samuel, "On a nonperturbative vacuum for the open bosonic string," Nucl. Phys. **B336** 263 (1990).

[7] A. Sen and B. Zwiebach, "Tachyon condensation in string field theory," JHEP **0003**, 002 (2000), hep-th/9912249.

[8] N. Moeller and W. Taylor, "Level truncation and the tachyon in open bosonic string field theory," Nucl. Phys. B **583**, 105 (2000), hep-th/0002237.

[9] S. B. Giddings, E. J. Martinec and E. Witten, "Modular Invariance In String Field Theory," Phys. Lett. B **176**, 362 (1986).

[10] B. Zwiebach, "A Proof That Witten's Open String Theory Gives A Single Cover Of Moduli Space," Commun. Math. Phys. **142**, 193 (1991).

[11] S. Giddings, "The Veneziano amplitude from interacting string field theory," Nucl. Phys. **B278** 242 (1986).

[12] J. H. Sloan, " The scattering amplitude for four off-shell tachyons from functional integrals," Nucl. Phys. **B302** 349 (1988).

[13] S. Samuel, "Covariant off-shell string amplitudes," Nucl. Phys. **B308** 285 (1988).

[14] D. Z. Freedman, S. B. Giddings, J. A. Shapiro and C. B. Thorn, "The Nonplanar One Loop Amplitude In Witten's String Field Theory," Nucl. Phys. B **298**, 253 (1988).

[15] W. Taylor, "D-brane effective field theory from string field theory," Nucl. Phys. B **585**, 171 (2000), hep-th/0001201.

[16] A. Leclair, M. E. Peskin and C. R. Preitschopf, "String field theory on the conformal plane (1, 2)" Nucl. Phys. **B317** 411, 464 (1989).

[17] M. R. Gaberdiel and B. Zwiebach, "Tensor constructions of open string theories 1., 2.," Nucl. Phys. **B505** 569 (1997), hep-th/9705038; Phys. Lett. **B410** 151 (1997), hep-th/9707051.

[18] D. J. Gross and A. Jevicki, "Operator formulation of interacting string field theory (I), (II)," Nucl. Phys. **B283** 1 (1987); Nucl. Phys. **B287** 225 (1987).

[19] E. Cremmer, A. Schwimmer and C. Thorn, "The vertex function in Witten's formulation of string field theory" Phys. Lett. **B179** 57 (1986).

[20] S. Samuel, "The physical and ghost vertices in Witten's string field theory," Phys. Lett. **B181** 255 (1986).

[21] N. Ohta, "Covariant interacting string field theory in the Fock space representation," Phys. Rev. **D34** (1986) 3785; Phys. Rev. **D35** (1987) 2627 (E).

[22] V. A. Kostelecky and R. Potting, "Analytical construction of a nonperturbative vacuum for the open bosonic string," Phys. Rev. D **63**, 046007 (2001), `hep-th/0008252`.

[23] G. Moore and W. Taylor, "The singular geometry of the sliver," JHEP **0201**, 004 (2002), `hep-th/0111069`; L. Rastelli, A. Sen and B. Zwiebach, "Star algebra spectroscopy," JHEP **0203**, 029 (2002), `hep-th/0111281`; K. Okuyama, "Ghost kinetic operator of vacuum string field theory," JHEP **0201**, 027 (2002), `hep-th/0201015`; B. Feng, Y. H. He and N. Moeller, "The spectrum of the Neumann matrix with zero modes," JHEP **0204**, 038 (2002), `hep-th/0202176`; "Zeeman spectroscopy of the star algebra," JHEP **0205**, 041 (2002), `hep-th/0203175`; B. Chen and F. L. Lin, "Star spectroscopy in the constant B field background," `hep-th/0203204`; D. M. Belov, "Diagonal representation of open string star and Moyal product," `hep-th/0204164`.

[24] V. A. Kostelecky and S. Samuel, "The static tachyon potential in the open bosonic string," Phys. Lett. **B207** 169 (1988).

[25] G. Veneziano, "Construction of a crossing-symmetric, Regge-behaved amplitude for linearly rising trajectories," Nuovo Cim. **57A** 190 (1968).

[26] J. A. Shapiro and C. B. Thorn, "Closed String - Open String Transitions And Witten's String Field Theory," Phys. Lett. B **194**, 43 (1987).

[27] N. Berkovits, "SuperPoincare invariant superstring field theory," Nucl. Phys. B **450**, 90 (1995) [Erratum-ibid. B **459**, 439 (1996)], `hep-th/9503099`; "A new approach to superstring field theory," Fortsch. Phys. **48**, 31 (2000), `hep-th/9912121`; "Review of open superstring field theory," `hep-th/0105230`; "The Ramond sector of open superstring field theory," JHEP **0111**, 047 (2001), `hep-th/0109100`.

[28] E. Witten, "Interacting field theory of open superstrings," Nucl. Phys. **B276** 291 (1986).

[29] I. Ya. Aref'eva, P. B. Medvedev and A. P. Zubarev, "Background formalism for superstring field theory," Phys. Lett. **B240** 356 (1990); "Tachyon condensation in cubic superstring field theory," `hep-th/0011117`.

[30] E. D'Hoker and D. H. Phong, "Two-loop superstrings. I-IV," Phys. Lett. B **529**, 241 (2002), `hep-th/0110247`; Nucl. Phys. B **636**, 3 (2002), `hep-th/0110283`; Nucl. Phys. B **636**, 61 (2002), `hep-th/0111016`; `hep-th/0111040`.

[31] A. Strominger, "Closed Strings In Open String Field Theory," Phys. Rev. Lett. **58**, 629 (1987); P. Yi, Nucl. Phys. B **550**, 214 (1999), `hep-th/9901159`; A. Sen, JHEP **9910**, 008 (1999), `hep-th/9909062`; O. Bergman, K. Hori and P. Yi, Nucl. Phys. B **580**, 289 (2000), `hep-th/0002223`; G. W. Gibbons, K. Hori and P. Yi, Nucl. Phys. B **596**, 136 (2001), `hep-th/0009061`; A. Sen, J. Math. Phys. **42**, 2844 (2001), `hep-th/0010240`; A. A. Gerasimov and S. L. Shatashvili, JHEP **0101**, 019 (2001), `hep-th/0011009`; M. Kleban, A. E. Lawrence and S. H. Shenker, Phys. Rev. D **64**, 066002 (2001), `hep-th/0012081`; S. L. Shatashvili,

hep-th/0105076; G. Moore and W. Taylor, JHEP **0201**, 004 (2002), hep-th/0111069; A. Hashimoto and N. Itzhaki, JHEP **0201**, 028 (2002), hep-th/0111092; D. Gaiotto, L. Rastelli, A. Sen and B. Zwiebach, hep-th/0111129.

[32] I. Ellwood and W. Taylor, "Open string field theory without open strings," Phys. Lett. B **512**, 181 (2001), hep-th/0103085.

[33] I. Ellwood, B. Feng, Y. H. He and N. Moeller, "The identity string field and the tachyon vacuum," JHEP **0107**, 016 (2001), hep-th/0105024.

[34] L. Rastelli, A. Sen and B. Zwiebach, "String field theory around the tachyon vacuum," hep-th/0012251; "Vacuum string field theory," hep-th/0106010.